ARTICLES

Dynamic Process of Water Sorption in a Thermoplastic Modified Epoxy Resin System

Liang Li, MoJun Liu, and Shanjun Li*

Department of Macromolecular Science and The Key Laboratory of Polymer Engineering Science, Fudan University, Shanghai, 200433, China

Received: September 3, 2003; In Final Form: February 10, 2004

In the present work, dynamic water sorption processes in a series of poly(ether imide) (PEI) modified diglycidyl ether bisphenol A/(4,4′-diaminodiphenyl)sulfone (DGEBA/DDS) systems were investigated. The clear picture of the existing state and the diffusion process of water molecules in the blends was first elucidated by two-dimensional (2D) correlation analysis (based on attenuated total reflection Fourier transfer infrared (ATR-FTIR) measurement), and the novel technique used here could be the most effective as well as convenient way to perform the dynamic analysis on such investigations. Furthermore, by means of scanning electron microscopy (SEM), the delicate relationship between dynamic water sorption behavior and the morphology resulting from phase separation was also discussed. Two states of water as free/bound water were found in the systems, the diffusion sequence of which suggested not only composite-dependence but also morphology-dependence.

1. Introduction

The behavior of water diffusion in epoxy networks is a fascinating focus that scientists have been caring about for a long time,[1−6] for excellent properties of epoxy materials will be greatly affected by the water absorbed and thus its potential use can be confined. Nowadays, at least two types of water molecules in the epoxy networks depicted as free/bound water have been generally conceived. Nevertheless, due to different experimental methods, the sequence of whether free water forms prior to bound water or not is argued, each with certain evidential phenomena. Apicella et al.[7] and Adamson[8] support that, in the initial stage of the sorption process, only the existence of free water is permitted, while Moy and Karasz[9] and Li et al.[10,11] hold the opposite position. However, the theories are all based on single-component networks, while in the practical application of epoxy resins, linear thermoplastic polymers are always added to improve the fragile nature of the matrix, which inevitably leads to phase separation and results in relatively complicated sorption behavior. Although Pethrick and co-workers have performed observations on the final state of water molecules in poly(ether sulfone) modified epoxy systems,[12] integrated studies on the dynamic sorption process have not been achieved so far.

Morphology resulting from phase separation is a newly induced factor that exists in blend systems. Virtually, its effect on water diffusion has not been revealed up to now. It is reasonable that water diffusion will first take place in continuous regions. While in co-continuous phase, whether water molecules will diffuse into different components randomly or not remains elusive.

Recently, the attenuated total reflection Fourier transfer infrared (ATR-FTIR) technique has been promptly developed to provide in situ measurements, by means of which reliable mass−time sorption curves and rich information of the polymer−water molecular interactions are available.[13−16] Besides, generalized two-dimensional (2D) IR spectroscopy, proposed by Noda,[17−20] is developed to analyze various types of spectral data often obtained under dynamic experiments. This novel method can handle spectral fluctuations as an arbitrary function of time or any other physical variables, and it is able to probe the specific order of certain events taking place with the development of a controlling physical variable, which will be of most significance in the dynamic analysis.[21−25] The technique was successfully applied later to the analysis of ATR spectra. Using 2D correlation analysis on ATR-FTIR spectra, water sorption behavior and the state of water molecules all can be studied.[10−11,26−28]

In the present work, we monitor the dynamic water sorption behavior in a series of different content polyetherimide (PEI) modified diglycidyl ether bisphenol A/(4,4′-diaminodiphenyl)-sulfone (DGEBA/DDS) systems by scanning electron microscopy and ATR-FTIR spectrometer. The specific water diffusion sequence is obtained, and the effect of the morphology on sorption behavior in the systems with phase separation is also put forward.

2. Experimental Section

2.1. Materials. The poly(ether imide) (PEI, $[\eta] = 0.73$, $T_g = 218$ °C) was synthesized in one step from bisphenol A dianhydride (BISA-DA) and 4,4-[1,3-phenylenebis(1-methylethylidene)]bisaniline (BISM-diamine) with stoichimetric ratio 1:0.98 (mole ratio) in *m*-cresol at 200 °C for 6 h.[29] The structure is depicted in Figure 1.

The cure agent (4,4′-diaminodiphenyl)sulfone (DDS) (Shanghai Third Reagent Factory) and the epoxy oligomer diglycidyl

* To whom correspondence should be addressed. Telephone: 86-21-65642865. Fax: 86-21-65640293. E-mail: sjli@fudan.edu.cn.

10.1021/jp036625b CCC: $27.50
Published on Web 03/19/2004

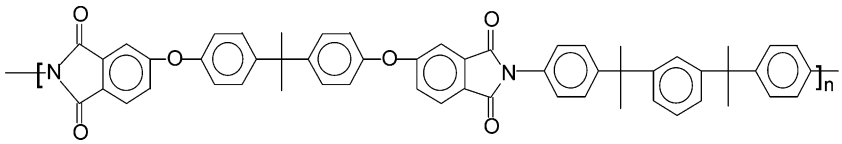

Figure 1. Chemical structure of PEI.

TABLE 1: Composition of Blends

blend code	DGEBA (weight)	PEI (weight)	DDS (weight)
EP	100	0	31
10-phr	100	10	31
15-phr	100	15	31
20-phr	100	20	31
PEI	0	100	0

ether bisphenol A (DGEBA) (DOW Chemical, Epon 828) were used without further purification.

The compositions of epoxy/PEI blends are listed in Table 1.

2.2. Film Preparation. The blend (EP, 10-phr, 15-phr, 20-phr, and PEI, respectively) (phr = pre hundred resin) and 31-phr DDS were dissolved in an appropriate amount of *N*,*N*-dimethylacetamide (DMAC) homogeneously with magnetic stirring. After evaporating in the oven for 24 h at 50 °C, the blends smeared over a carry glass sheet were cured in the vacuum oven at 180 °C/3 h and postcured at 200 °C/2 h. Then the films were peeled off and put in the vacuum oven at 70 °C for 5 days and finally cooled slowly down to room temperature. The thicknesses of the sample films were in the range of 30−40 μm, which were measured by a Coaest-1000(UK) nonferrous digital coating thickness gauge.

2.3. Scanning Electron Microscopy (SEM). The morphologies of impact fraction surfaces of samples were observed using a PhilipXL39 SCM. The fraction surfaces were coated with a layer of gold about 200 Å thick.

2.4. Diffusion Measurements by Time-Resolved ATR−FTIR. ATR-FTIR measurements were performed at 24 °C using a Nicolet Nexus Smart ARK FTIR spectrometer equipped with a DTGS-KBr detector, solid cell accessories, and a ZnSe internal reflection element (IRE) crystal. The spectra were measured at 4 cm^{-1} resolution and eight scans, and the wavenumber range was 650−4000 cm^{-1}. The film-covered IRE crystal with a filter paper above the sample film was mounted in an ATR cell, and the spectra of the dry film was collected as background spectra; then without moving the sample, distilled water was injected into the filter paper while starting the data acquisition by a macro program. A typical sorption loop lasted about 15 min with an acquisition time interval of 27 s. The ATR-FTIR spectra in two wavenumber ranges of sorbed water in specimens were obtained from subtraction spectra of the background and the wet sample films.

2.5. Two-Dimensional Correlation Analysis. Six spectra at equal time intervals in a certain wavenumber range were selected for 2D correlation analysis using the software "2D Pocha", which was composed by Daisuke Adachi (Kwansei Gakuin University).[30,31] A time-averaged reference spectrum was shown at the side and top of the 2D correlation maps for comparison. In the 2D correlation maps unshaded regions indicate positive correlation intensities, while shaded regions indicate negative correlation intensities.

3. Results and Discussion

3.1. Morphology from Scanning Electron Microscopy. Morphologies from SEM are presented in Figure 2.

For 10-phr, the dispersed phase is observed with the occluded PEI regions, while for 15-phr and 20-phr, co-continuous phases

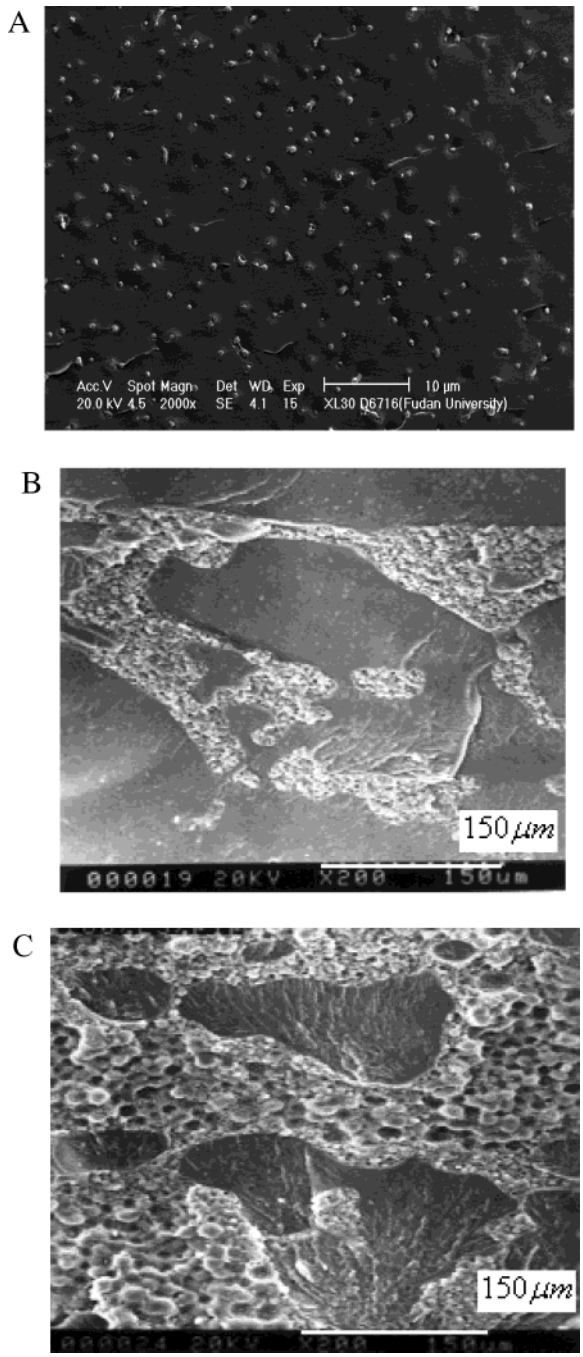

Figure 2. SEM phase structures: (A) 10-phr; (B) 15-phr; (C) 20-phr.

are presented, which is consistent with the increasing PEI content and requires no further interpretation.

3.2. Dynamic Water Sorption Process from 2D Correlation Analysis. According to 2D correlation analysis, the synchronous correlation spectra ranging from 2800 to 3700 cm^{-1} of different thermoplastic content systems are shown in Figure 3. In the reference spectra at the top and side of the 2D correlation maps, two main bands in the ranges of 3200−3600 and 2900−3000 cm^{-1} are assigned to water OH stretching vibration and bulk CH vibration, respectively.

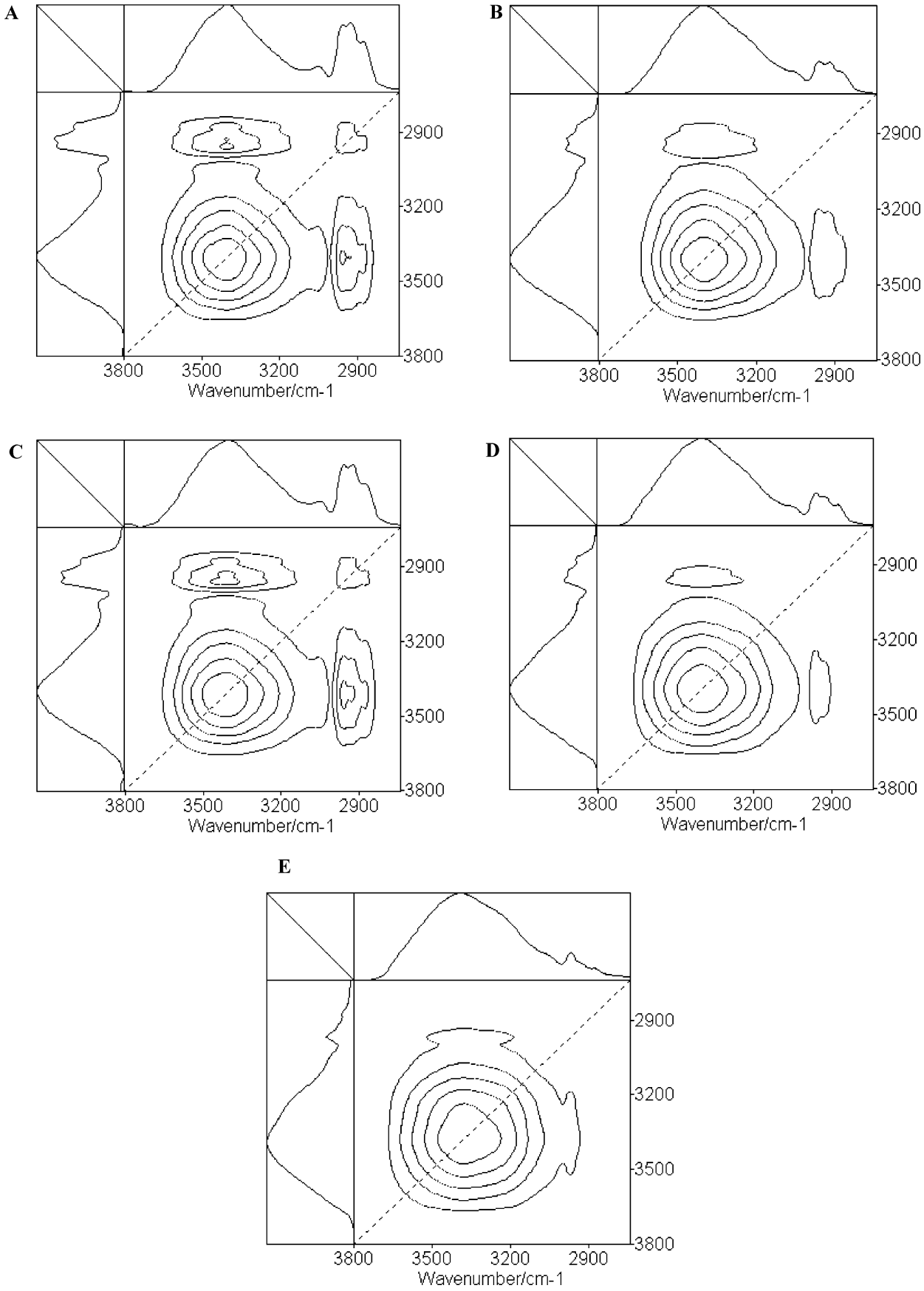

Figure 3. Synchronous 2D correlation spectra of water at 2800−3700 cm^{-1}: (A) EP; (B) 10-phr; (C) 15-phr; (D) 20-phr; (E) PEI.

In the corresponding asynchronous correlation spectra shown in Figure 4, water vibration bands at 3200−3600 cm^{-1} that overlap in the original FTIR spectra are split into two separate bands ν_1,ν_2, whose wavenumbers are reported in Table 2.

The two components corresponded to the absorbance from the strongly hydrogen-bonded and less hydrogen-bonded hydroxyl groups, respectively. Thus, the phenomenon indicates two different states of water in these systems. The bands at

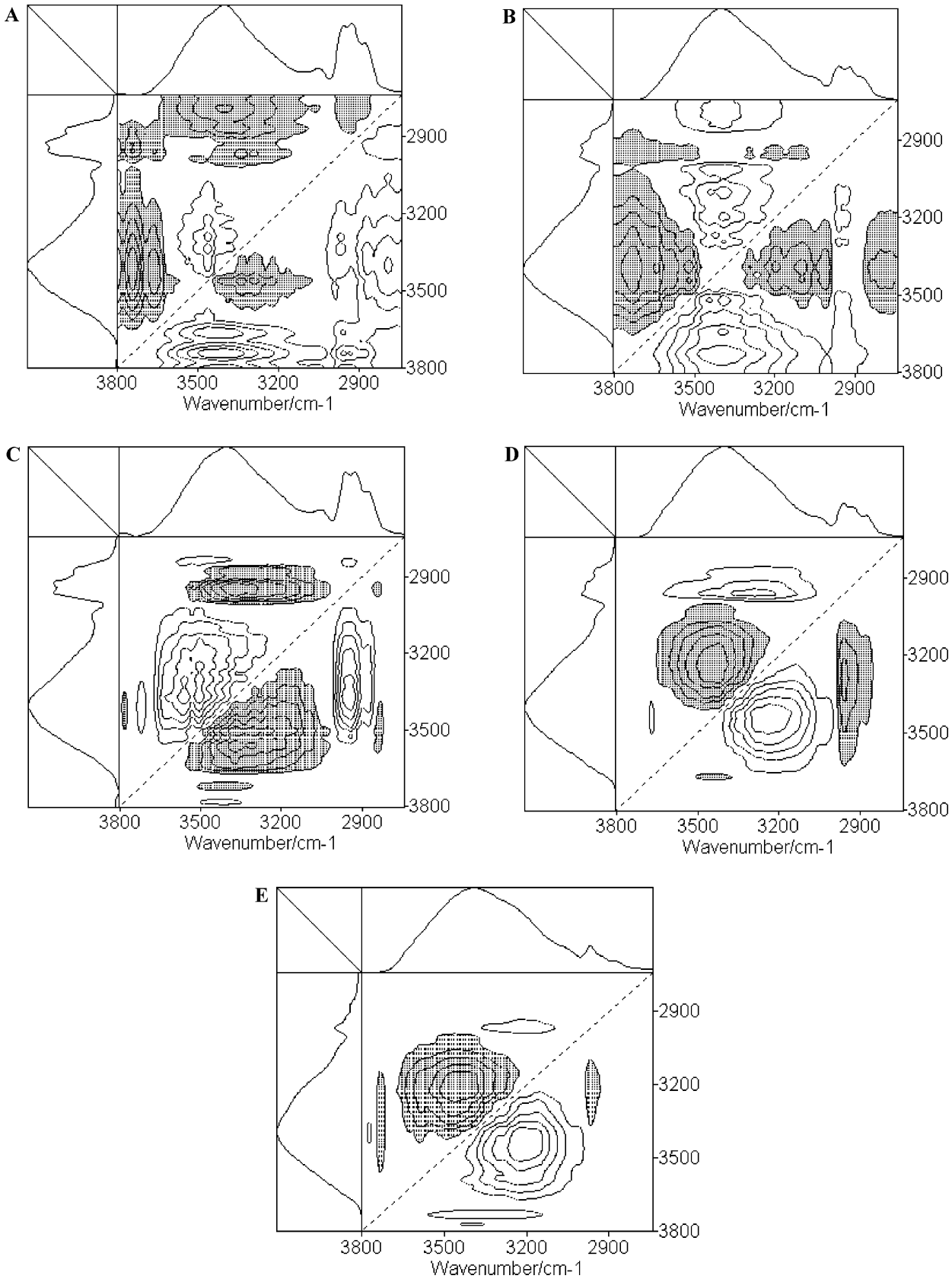

Figure 4. Asynchronous 2D correlation spectra of water at 2800−3700 cm^{-1}: (A) EP; (B) 10-phr; (C) 15-phr; (D) 20-phr; (E) PEI.

higher wavenumber can be water molecules distributed into free volume (microvoids) or molecularly dispersed with less hydrogen bonding (bulk dissolve),[10,11] while bands at lower wavenumber reveal the stronger hydrogen bonding interaction between hydroxyl groups of epoxy networks and water molecules. [10,11]

As shown in Table 2, the wavenumbers of the OH band from bound water (ν_2) in 10-phr, 20-phr, and PEI are all lower than that in EP, which implies the strength of the hydrogen bonding between water molecules and epoxy networks is distinctly reinforced by adding the PEI component. However, the weakest hydrogen bonding is observed around the beginning of the co-

TABLE 2: Wavenumbers of Separate Bands from Asynchronous Correlation

	EP	10-phr	15-phr	20-phr	PEI
ν_1	3465	3394	3509	3444	3450
ν_2	3294	3143	3311	3228	3203

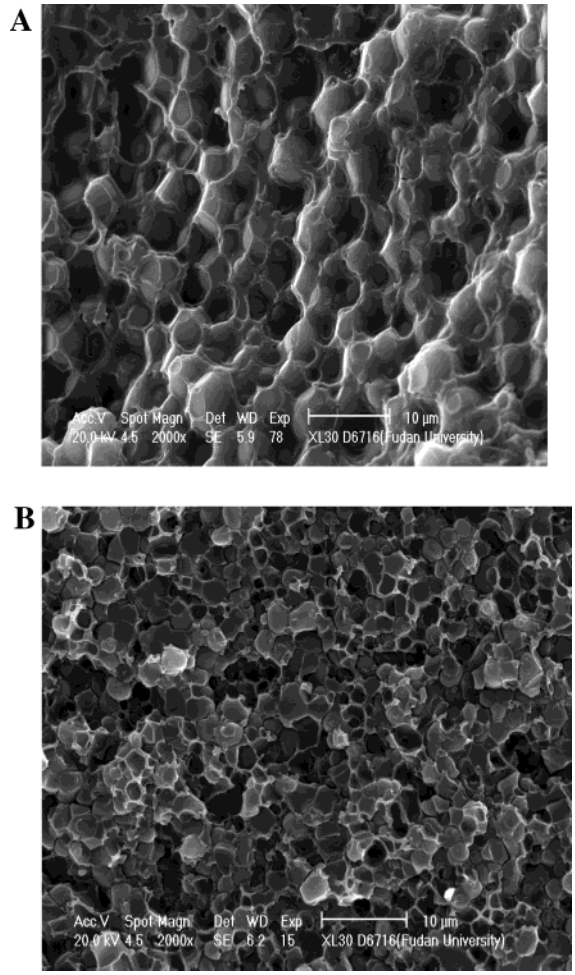

Figure 5. SEM phase morphologies of (A) 15-phr and (B) 20-phr.

continuous phase (15-phr), at which stage anomalous water sorption behavior is also noticed in PES-modified epoxy resins.[12] Pethrick et al. attribute the abnormity to polarization phenomenon associated with the microporous structure of the surface, which could also be the case here.

Additionally, the sign of the asynchronous correlation peak $\Psi(\nu_1,\nu_2)$ gives information about the sequential order of the intensity changes between band ν_1 and band ν_2. According to the publications of Noda,[17] if $\nu_1 > \nu_2$ and the sign of the asynchronous band $\Psi(\nu_1,\nu_2)$ is positive (unshaded area), band ν_1 varies prior to band ν_2, while the negative asynchronous band (shaded area) implies the opposite phenomena. Take Figure 4D for example; the negative band $\Psi(3444,3228)$ reveals that the change of the population of the strong hydrogen bonded OH species (3228 cm^{-1}) occurs earlier than the change of the population of the weak hydrogen bonded OH species (3444 cm^{-1}). So in the case of 20-phr, the bound water forming stronger hydrogen bonding with epoxy networks is produced prior to the water diffused into free volume (microvoids) or water molecularly dispersed with less hydrogen bonding (bulk dissolve). The same results of PEI and conversed phenomenon in EP, 10-phr, and 15-phr are obtained.

The conclusion can be drawn that, in the process of water diffusion, for EP, 10-phr, and 15-phr, diffusion of water molecules into free volume occurs prior to the interaction between water molecules with specific hydrophilic groups, while, for 20-phr and PEI, the sequence is changed conversely.

Furthermore, the asynchronous correlation spectra of EP, 10-phr, and 15-phr is similar to each other, which suggests that, in 10-phr and 15-phr, water molecules first diffuse into epoxy regions and then into PEI regions. From the comparison of the asynchronous correlation spectra of 20-phr and PEI, the deduction can be derived that in 20-phr water molecules first diffuse into PEI regions.

According to the SEM result (Figure 2A), it is reasonable that water molecules will first diffuse into continuous regions in the case of 10-phr. However, water diffusion in the co-continuous phase will not treat the different components in the same way, and opposite sequences both have been found. To further investigate the subtle difference in the morphology of blends in the co-continuous phase, Figure 5 is presented by amplifying the microdomains of Figure 2B,C.

Clearly, in both cases the epoxy regions are all occluded by PEI continuous phase. In 15-phr, particularly, they are wrapped more completely as well as tightly. As a result, in the case of 15-phr, water diffusion paths in tightly compacted epoxy regions may be narrowed and a long percolation path between the two components may be generated, which could be responsible for the opposite water diffusion sequence compared with that in 20-phr.

4. Conclusion

Clear pictures of water diffusion processes in a series PEI-modified DGEBA/DDS systems are elucidated here by ATR-FTIR experiments with 2D correlation analysis, which could be the most effective as well as convenient way to perform the dynamic analysis on such investigations.

Two types of water molecules with strong/weak hydrogen bonding have been found in all the systems studied here, which can be regarded as bound/free water. However, the process of water diffusion in different systems will not always share similar characteristics. For EP, 10-phr, and 15-phr, diffusion of water molecules into free volume occurs prior to the interaction between water molecules with specific hydrophilic groups. However, for 20-phr and PEI, the sequence is changed conversely. By means of scanning electron microscopy (SEM), the delicate relationship between dynamic water sorption behavior and the morphology resulting from phase separation is also discussed. Accordingly, attributed to the specific morphology, for 10-phr and 15-phr, water molecules first diffuse into an epoxy-rich phase and then into the PEI-rich phase, while, for 20-phr, the phenomenon is just the opposite. Therefore, the diffusion sequence of free/bound water suggests not only composite-dependence but also morphology-dependence.

Acknowledgment. We gratefully acknowledge the financial support of this research by the National Science Foundation of China (NSFC; Grant No. 50273007).

References and Notes

(1) Aronhime, M. T.; Gillham, J. K. *J. Appl. Polym. Sci.* **1986**, *32*, 3589.

(2) Lucas, J. P.; Zhou, J. M. *Macromol. Compos. Sci. Technol.* **1995**, *53*, 57.

(3) Zhou, J. M.; Lucas, J. P. *Polymer* **1999**, *40*, 5505.

(4) Núñez, L.; Villanueva, M.; Fraga, F.; Núñez, M. R. *J. Appl. Polym. Sci.* **1999**, *74*, 353.

(5) Xiao, G. Z.; Shanahan, M. E. R. *J. Polym. Sci., Part B: Polym. Phys.* **1997**, *35*, 2659.

(6) Xiao, G. Z.; Shanahan, M. E. R. *J. Appl. Polym. Sci.* **1997**, *65*, 449.
(7) Apicella, A.; Nicolais, L.; De cataldis, C. *J. Membr. Sci.* **1985**, *18*, 211.
(8) Adamson, M. *J. Mater. Sci*. **1980**, *15*, 1736.
(9) Moy, P.; Karasz, F. E. *Polym. Eng. Sci.* **1980**, *20*, 315.
(10) Liu, M. J.; Wu, P. Y.; Ding, Y. F.; Chen, G.; Li, S. J. *Macromolecules* **2002**, *35*, 5500.
(11) Liu, M. J.; Wu, P. Y.; Ding, Y. F.; Chen, G.; Li, S. J. *Phys. Chem. Chem. Phys*. **2003**, *5*, 1848.
(12) Pethrick, R. A.; Hollins, E. A.; McEwan, I.; MacKinnon, A. J.; Cannon, L. A.; Jenkins, S. D.; Mcgrail, P. T. *Macromolecules* **1996**, *29*, 5208.
(13) Macia, R.; Jack, Y. *J. Chem. Soc*. **1996**, *92*, 2731.
(14) Fieldson, G. T.; Barbari, T. A. *Polymer* **1993**, *34*, 1193.
(15) Marechal, Y.; Chamel, A. *J. Phys. Chem*. **1996**, *100*, 8551; *Faraday Discuss*. **1996**, *103*, 349.
(16) Cotugno, S.; Larobina, D.; Mensitieri, G.; Musto, P.; Ragosta, G. *Polymer* **2001**, *42*, 6431.
(17) Noda, I. *Appl. Spectrosc.* **1993**, *47*, 1329.
(18) Noda, I. *Bull. Am. Phys. Soc.* **1986**, *31*, 520.
(19) Noda, I. *J. Am. Chem. Soc*. **1989**, *111*, 8116.
(20) Noda, I. *Appl. Spectrosc.* **1990**, *44*, 550.
(21) Czarnecki, M. A.; Wu, P.; Siesler, W. H. *Chem. Phys. Lett*. **1998**, *283*, 326.
(22) Liu, Y.; Ozaki, Y.; Noda, I. *J. Phys. Chem*. **1996**, *100*, 7327.
(23) Ozaki, Y.; Liu, Y.; Noda, I. *Macromolecules* **1997**, *30*, 2391.
(24) Czarnecki, M. A.; Maeda, H.; Ozaki, Y.; Suzuki, M.; Iwahashi, M. *J. Phys. Chem. A* **1998**, *102*, 6655.
(25) Ren, Y.; Shimoyama, K.; Ninomiya, T.; Matsukawa, K.; Inoue, H.; Noda, I.; Ozaki, Y. *Appl. Spectrosc.* **1999**, *53*, 919.
(26) Wu, P.; Siesler, H. W. *Chem. Phys. Lett.* **2003**, *374*, 74.
(27) Shen, Y.; Wu, P. *J. Phys. Chem. B* **2003**, *107*, 4224.
(28) Peng, Y.; Wu, P.; Siesler, H. W. *Biomacromolecules* **2003**, *4*, 1041.
(29) Cui, J.; Chen, J.; Zhang, Z. Z.; Li, S. J. *Macromol. Chem. Phys.* **1997**, *198*, 1865.
(30) Katsumoto, Y.; Adachi, D.; Sato, H.; Ozaki, Y. *J. Near Infrared Spectrosc.* **2002**, *10*, 85.
(31) Adachi, D.; Katsumoto, Y.; Sato, H.; Ozaki, Y. *Appl. Spectrosc.* **2002**, *56*, 357.